Statistical Thermodynamic Approach for Evaluating the Writhe Transformations in Circular DNAs

C. Anselmi,[†] G. Bocchinfuso,[†] P. De Santis,*[,†] M. Fuà,[†] A. Scipioni,[†] and M. Savino[‡]

Dipartimento di Chimica and Dipartimento di Genetica e Biologia Molecolare, Istituto Pasteur, Fondazione Cenci Bolognetti−Università di Roma "La Sapienza", 00185 Roma, Italy

Received: March 18, 1998

The model we advanced in a previous paper about DNA circularization (*J. Phys. Chem.* **1996**, *100*, 9968−9976), is extended to the sequence-dependent equilibrium between relaxed and supercoiled forms of circular DNAs. In the framework of first-order elasticity, we evaluate the canonical ensemble partition function and the related thermodynamic properties in terms of continuous variations of writhing and linking numbers, giving an estimate of the writhe transitions. The comparison with the Monte Carlo results is very significant. It convincingly proves the validity of the proposed model as a favorable alternative to computationally heavy Monte Carlo simulations. Moreover the model is suitable to study the sequence-dependent effects in the writhe transitions and offers good perspectives for further developments.

Introduction

Circular and looping DNAs are important in many fundamental biological processes; they represent topological domains, where the local events and perturbations, due to the interactions with different kinds of molecules, are integrated and lead to relevant superstructural transformations.[1−4] Since the DNA supercoiling discovery, a great effort has been devoted to theoretical studies on circular and looping DNA to investigate the superstructural changes that occur by increasing the magnitude of the linking number. Both analytical and numerical strategies were adopted to obtain the minimum energy structures of small circular filaments as a function of the linking difference. Several authors investigated the twist and writhe transitions of topologically constrained circular DNAs. In 1977 Benham[5] advanced the first elastic model to explain the supercoiling transformations occurring in circular DNAs. In 1979 Le Bret,[6,7] adopting a model based on first-order elasticity, solved the problem of finding the whole minimum energy pathway for the open circular to figure-8 form transition induced by twisting deformations in the ideal case of a straight rodlike elastic DNA. He found that the circle is destabilized when the twisting number becomes greater than $\sqrt{3}$ times the ratio between the bending and twisting force constants, independently of the DNA length.

In 1985 Shimada and Yamakawa[8] applied Monte Carlo methods to the case of a twisted wormlike chain to explain the breadth of the experimental Gaussian distribution of topoisomers with different linking numbers. In 1986 Levene and Crothers[9] obtained an estimate of the torsional DNA rigidity adopting Monte Carlo methods. Olson,[10] Hao and Olson,[11] Schlick et al.,[12] and Westcott et al.[13] investigated the supercoiling and the looping of DNA as a thin isotropic elastic rod and more recently attempted to study the effect of the sequence-directed bending using the numerical analysis and the elasticity theory. In particular Schlick et al.[12] first mentioned higher order transitions.

Bauer and co-workers[14,15] used the finite element analysis to evaluate the dependence of the writhing and the twisting upon the linking number difference in discretely or uniformly bent DNAs. They found that it is strongly influenced by intrinsic bends.

A general conclusion of these investigations was the existence of a catastrophic transition between the relaxed and supercoiled forms of a circular DNA in response to the twisting deformations; this conclusion can be extended to looping DNAs.

More recently, some criticism has been raised against mechanical models because the predicted transitions would have a physical meaning only at the low-temperature limit when the energy fluctuations and the related entropy can be neglected. In order to overcome this problem, Gebe and Schurr[16] used Monte Carlo simulations to investigate the first transition in writhe of a circular filament representing a 468 base pair (bp) uniform idealized DNA. Adopting twisting and bending elastic parameters and an appropriate model of the Poisson−Boltzmann potential for the electrostatic contributions of a cylindrical wormlike DNA with a linear charge density, they obtained the mean free energy and internal energy changes versus the writhe (W) for different values (from 0 to 2.25 turns) of the linking number difference (ΔL). From these functions they easily calculated the ΔL value that induces the transformation between the open circular and the figure-8 form. It was significantly lower and the transformation smoother than that predicted by simple mechanical models. The importance of considering thermodynamic ensembles instead of mechanistic energy minimization was also stressed by Sprous et al.[17] using molecular dynamics simulations. They examined both ideal homogeneous DNA and curved DNA, reaching the conclusion that the average and dynamic properties are affected by both DNA sequence and size.

Marko and Siggia[18] have recently developed a statistical mechanical theory for long superhelical wormlike DNAs that

* To whom correspondence should be addressed. Phone: 39 6 49913730. Fax: 39 6 4453827. E-mail: p.desantis@caspur.it.
[†] Dipartimento di Chimica.
[‡] Dipartimento di Genetica e Biologia Molecolare.

S1089-5647(98)01552-1 CCC: $15.00 © 1998 American Chemical Society
Published on Web 06/25/1998

includes entropy contributions in the equilibrium configuration of the elastic chains.

However, it is known that DNA circularization is strongly dependent on the sequence also for DNAs of several hundreds base pairs. Therefore it is plausible that also the transitions between relaxed and supercoiled forms should be sequence directed. This was first proved by Laundon and Griffith[19] by electron microscopy experiments. They showed that curved DNA tracts, cloned into a plasmid, were segregated at the turn regions of the supercoiled forms induced by girase.

This can be relevant for the control of the gene expression that often depends on bringing together DNA sequences separated by considerable distance (up to several hundred base pairs) along the double helix, e.g., supercoiled DNA template that facilitates loop formation in the *lac* and *ara* repressors.[20]

Klenin et al.[21] have recently made Monte Carlo simulations to study the effects of curved sequences on the structure of long superhelical DNAs. They generated an equilibrium ensemble of a 2700 bp DNA chain at high supercoiling density ($\Delta L = -15$) with one or two 120° bends inserted at different relative positions. They found the bends segregated at the loops of superhelices (linear and branched), as experimentally found by Laundon and Griffith.[19]

More recently, Chirico and Langowski[22] presented Brownian dynamics simulations to analyze the effect of a permanent bend on the structure and the dynamics of a 1870 bp superhelix with $\Delta L = -10$, proving that a permanent bend drastically changes the superstructure and the internal motions of the DNA.

However, these simulations are computationally heavy and do not appear to have good perspectives of further development at present.

To approach the problem of the sequence-dependent writhe transformations, we have developed the simple elastic model we successfully adopted in a previous paper[23] to predict the sequence-dependent circularization propensity of DNA, to obtain an analytical solution for the first and second writhe transition in the case of small-sized DNAs (bp < 1000). The comparison with the Monte Carlo results obtained by Gebe and Schurr[16] and Schlick et al.[12] is very significant and convincingly proves the validity of the proposed model.

Calculation of the Ground-State Free Energy of a Circular DNA When the Writhe Changes under Elastic Twisting Stress

The three-dimensional superstructure of a DNA chain can be conveniently expressed as a curvature function representing the directional change of the DNA axis between the *n*th and the (*n*+1)th base pairs in the complex plane.[24]

Let $\mathbf{C}(n)$ be the curvature function of a circular DNA along the sequence number, *n*, implicitly characterized by the integral linking number *L* and writhing number *W* (the twisting number is obviously $L - W$). Adopting our model of DNA curvature,[23-27] $\mathbf{C}(n)$ is represented as a complex function of the sequence number *n* (in radians per bp):

$$\mathbf{C}(n) = \frac{\pi}{180\nu} \sum_{n\text{th turn}} \mathbf{d}(s) \exp(2\pi i s/\nu) \qquad (1)$$

ν is the helical periodicity of the DNA tract evaluated from the corresponding twist angles (Ω), and $\mathbf{d}(s) = \rho - i\tau$ is the local deviation of the recurrent dinucleotide steps from the canonical B-DNA structure in terms of the roll (ρ) and tilt (τ) angles (in degrees) (see Figure 1).

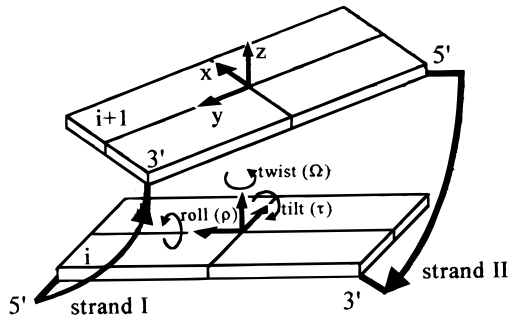

Figure 1. Orientational parameters of the base pair average plane in a dinucleotide step.

$\mathbf{C}(n)$ can be developed in terms of Fourier amplitudes as

$$\mathbf{C}(n) = \frac{1}{N} \sum_{j=-N/2}^{N/2} \mathbf{A}(j) \exp(2\pi i n/Nj) \qquad (2)$$

where *N* is the bp number and

$$\mathbf{A}(j) = \sum_{n=1}^{N} \mathbf{C}(n) \exp(-2\pi i n/Nj) \qquad (3)$$

For the shift theorem,[28] the Fourier amplitudes of the curvature function that represents the circular DNA after a uniform twisting along its axis are shifted in their frequencies by the twisting number difference (ΔT):

$$\mathbf{A}(j + \Delta T) = \sum_{n=1}^{N} (\mathbf{C}(n) \exp(2\pi i n/N\Delta T)) \exp(-2\pi i n/N(j + \Delta T)) \qquad (4)$$

In fact, in our curvature representation, a uniform twisting of ΔT around the local DNA axes is equivalent to multiplying the curvature function by $\exp(2\pi i n/N\Delta T)$ along the sequence number.

For this reason, the amplitudes $\mathbf{A}(j + \Delta T)$ represent a DNA superstructure whose curvature has the same modulus with respect to that corresponding to the $\mathbf{A}(j)$ series, but the phase uniformly increased with $\Delta T/N$ along the sequence.

This transformation does not generally ensure the circularization integrity; nevertheless, to correctly seal the DNA strands, it is sufficient to refine the moduli of the Fourier amplitudes (this preserves the twisting) that are directly involved in circularization. This is obtained adopting a steepest descent algorithm that quickly converges.

Finally, we obtain a new curvature function (by inverse Fourier transform) which represents a different form of the circular DNA characterized by a writhing number *W* (that is equivalent to $-\Delta T$ at constant linking number, *L*).

For example, consider a figure-8 form of an intrinsically straight DNA. As shown in the Appendix, this form has a curvature function characterized by two Fourier terms of frequency +1 and −1 and moduli both equal to 2.405π. If we imagine twisting the DNA chain around its axis by an angle, i.e. 0.1 turns, uniformly distributed along the sequence, we will obtain a new form characterized by two Fourier terms whose moduli are still equal to 2.405π, but with their frequencies shifted to 1.1 and −0.9.

The shape obtained is now open, but we can change the moduli of the two amplitudes to eliminate the end-to-end distance. Since changing the amplitudes does not affect the twisting, the new shape will still differ by 0.1 twisting number

from the figure-8 form; therefore, when it reaches the correct circular form, its writhing number will differ by −0.1; it will then have $W = 0.9$. This was verified by direct writhing number calculations using the Calagareanu[29] discretized form of the Gauss integral:

$$W = \frac{1}{4\pi} \sum_{i,j=1}^{N} \frac{\mathbf{I}_i \times \mathbf{I}_j \cdot \mathbf{r}_{ji}}{|\mathbf{r}_{ji}|^3} \tag{5}$$

where $\mathbf{l}_i$ and $\mathbf{l}_j$ represent the unit elements of the DNA axis and $\mathbf{r}_{ji}$ is their vectorial distance.

As a result, we can easily obtain the Fourier representation of circular DNAs as a function of W, on account of the topological equivalence between ΔT and $-W$:

$$\mathbf{A}(j - W) = \mathbf{A}(j + \Delta T) \tag{6}$$

In order to select the ground-state conformation of a circular DNA for each writhing number, we have to minimize the square average deviation between the curvature of the circular form and the intrinsic curvature of the linear form that is equivalent to minimize the elastic energy. Using the Parseval equality,[30] this can be conveniently expressed in terms of the summation of the squared Fourier amplitude differences:

$$\langle |\Delta \mathbf{C}(n)|^2 \rangle_W = \frac{1}{N^2} \sum_{j=-N/2}^{N/2} |\Delta \mathbf{A}(j - W)|^2 \tag{7}$$

The subscript W indicates the writhing constant average over the sequence. If we maintain invariant all the amplitudes that characterize the intrinsic linear form, except those conditioned by the writhing number and the circularization constraints, we obtain the least-squared average curvature deviation, corresponding to the ground state of the bending elastic energy. As a result,

$$E_b^\circ(W) = \frac{1}{2} Nb \langle |\Delta \mathbf{C}(n)|^2 \rangle_W = \frac{b}{2N} \sum_k \Delta A^\circ(k - W)^2 \tag{8}$$

The summation extends over the k constrained $\Delta \mathbf{A}^\circ(k - W)$ as the others are equal to zero. $\Delta A^\circ(k - W)$ (italic) represents the modulus of $\Delta \mathbf{A}^\circ(k - W)$ (bold) (this convention will be used in the whole paper). b represents the apparent isotropic bending force constant (it is related to the persistence length P and the monomer repeat h (3.4 Å) by $b = P/(h\beta)$, $\beta = 1/(k_B T)$, k_B, the Boltzmann constant).

Similarly, the twisting energy can be expressed as

$$E_t^\circ(W, \Delta L) = \frac{1}{2} Nt \langle \Delta \Omega^2 \rangle_{W, \Delta L} = \frac{t}{2N} \sum_j \Delta B(j)^2 \tag{9}$$

where t represents the apparent twisting force constant (it is related to the torsional rigidity, C, by $t = C/h$); $\Delta\Omega$ is the deviation from the intrinsic dinucleotide twist (in radians) and $\Delta B(j)$ are the corresponding Fourier amplitude differences. ΔL represents the difference between the linking number of the circular forms which must be an integer, and the sequence-dependent intrinsic twisting number of the linear DNA. It remains a topological invariant under changes of twisting and writhing numbers. This definition has been proposed by different authors and is adopted in the present paper for an easy comparison of the results. Therefore ΔL can assume different fractional values for different sequences, also for an equal number of base pairs, when intrinsic twist differences exist.

However, the topological condition $\Delta L = \Delta T + W$ constrains $\Delta B(0)$ to assume the value equal to $2\pi\Delta T = 2\pi(\Delta L - W)$, whereas the remaining $\Delta B(j)$ should be zero if, as for the bending energy, we assume the equivalence of all the pertinent amplitudes of the linear and the circular forms except $\mathbf{B}(0)$. Therefore, the ground-state elastic energy becomes

$$E^\circ(W, \Delta L) = \frac{b}{2N} \sum_k \Delta \mathbf{A}^\circ(k - W)^2 + \frac{t}{2N} [2\pi(\Delta L - W)]^2 \tag{10}$$

All the remaining energy contributions arising from water molecules and counterions interactions are considered to be invariant with respect to writhe transformations (at least for a low supercoiling density) that involve only slight changes of the dinucleotide structure. Furthermore, bending and twisting force constants we adopted are empirical values and implicitly contain a relevant amount of these contributions. This is not true for macrocounterions as proteins, whose interactions extend over many nucleotide steps and therefore are capable of recognizing DNA superstructures.

As a result, in our model writhe changes and dynamic fluctuations practically occur in a constant external force field and are only driven by the internal elastic potential (at least for the first writhe transition).

This approximation works very satisfactorily in predicting the DNA sequence-dependent circularization propensity as shown in a previous paper.[23] Here we follow the same strategy to define the constrained amplitudes for writhing numbers continuously changing from −2 to 2.

Evaluation of the Ground-State Free Energy of an Intrinsically Straight DNA

We first considered the case of a uniform (or random) DNA sequence characterized by the absence of an intrinsic curvature that corresponds to having a Fourier spectrum identically zero. In this case we have previously shown that it is enough to set $A(0) = 2\pi$ for the correct circularization. Similarly it is easy to show (see Appendix) that the amplitudes we must consider for the structure with writhing number $W = 1$ (figure-8 form) are $A(1) = A(-1) = 2.405\pi$. Actually, the figure-8 form so obtained is planar, but the elastic energy required to take into account the excluded volume at the crossing region is not significant for DNAs containing at least a few hundred base pairs. Finally, for supercoiled DNAs with $W = 2$ (neglecting the excluded volume), the planar form is characterized by $A(0) = 2\pi$ and $A(2) = A(-2) = 2.41\pi$. The last condition corresponds to the minimum bending energy contribution of the $\mathbf{A}(2)$ and $\mathbf{A}(-2)$ that allows a formally planar supercoiled form with a double crossing. Also in this case, the elastic energy required to take into account the excluded volume at the crossing regions can be neglected in first approximation.

In fact, we have considered the problem of the excluded volume using optimization methods and adopting a DNA effective diameter 2 times the geometrical value to avoid the fluctuation suppression[18] and in agreement with simulations.[31] Figure 2 diagrammatically reports the optimized amplitudes in the range of writhing number 0−2 (the diagram for negative values is symmetrically related) for a circular DNA with 450 bp; however, for longer sequences the diagram significantly changes only in a closed region about $W = 1$, where the crossing of $A^\circ(-W)$ and $A^\circ(2 - W)$, as well as the onset of $A^\circ(4 - W)$, progressively shifts toward $W = 1$ as a result of the excluded volume of the figure-8 form. As an example, Figure 3 shows

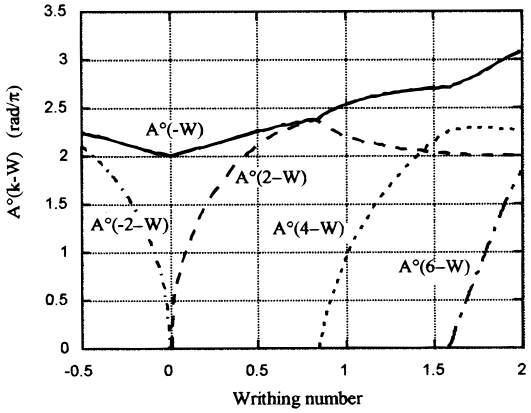

Figure 2. Values of the constrained Fourier amplitudes vs the writhing number (the diagram for negative writhes is symmetrically related).

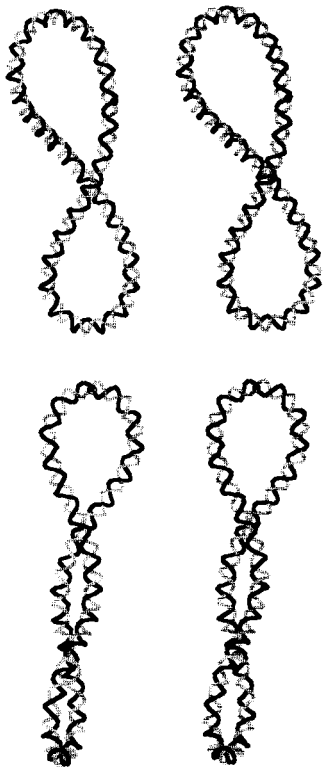

Figure 3. Stereoprojections of the ground-state superstructures with writhing numbers 1.0 (top) and 1.5 (bottom).

the stereoprojections of two superstructures with writhing numbers 1.0 and 1.5.

Adopting the amplitudes reported in Figure 2 and eq 10, it is easy to obtain the ground state for different W and ΔL and calculate the elastic energy.

$$E°(W,\Delta L) = b/(2N)[A°(-W)^2 + A°(2 - W)^2 + A°(4 - W)^2] + t/(2N)[2\pi(\Delta L - W)]^2 \quad (11)$$

These calculations were first performed for a wormlike 468 bp DNA, adopting the same bending and twisting force constants of Gebe and Schurr (corresponding to a persistence length $P =$ 500 Å and a torsional rigidity $C = 2.0 \times 10^{-19}$ erg cm) to try a comparison with their Monte Carlo data.[16]

The results are very significant, as illustrated in Figure 4, where the Monte Carlo mean internal energy is compared with the theoretical ground-state elastic energy. The two sets of values differ by a strictly constant energy contribution ($48/\beta$)

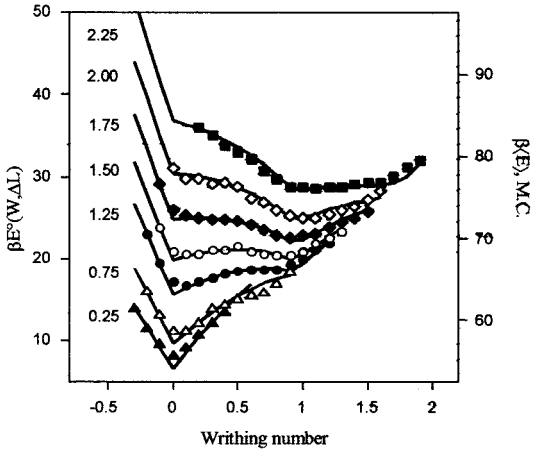

Figure 4. Ground-state first-order elastic energy ($E°$) (solid lines) of a uniform 468 bp DNA vs the writhing number (W) for different linking number differences (ΔL). The same bending and twisting force constants of Gebe and Schurr (corresponding to a persistence length $P = 500$ Å and a torsional rigidity $C = 2.0 \times 10^{-19}$ erg cm) were adopted for a comparison with the mean internal energy $\langle E \rangle$ (different symbols) of their Monte Carlo simulations.[16]

that clearly indicates the equivalence of the electrostatic and solvent interactions as well as of the energy fluctuations when W and ΔL change (or less likely, a sort of compensation of these two energy contributions).

In order to evaluate the degeneration of the ground state as a function of the writhing number, we have analyzed the dependence among the phases ϕ of the constrained amplitudes: $\mathbf{A}°(-W)$, $\mathbf{A}°(2 - W)$, and $\mathbf{A}°(4 - W)$ (see Figure 2).

In fact, the curvature $\mathbf{C}(n)$ of the circular forms changes with the constrained amplitude phases as

$$\mathbf{C}(n) = \frac{1}{N}\left\{A°(2 - W)\exp\left[2\pi i\left[\frac{n}{N}(2 - W) + \phi(2 - W)\right]\right] + A°(-W)\exp\left[2\pi i\left[\frac{n}{N}(-W) + \phi(-W)\right]\right] + A°(4 - W) \times \exp\left[2\pi i\left[\frac{n}{N}(4 - W) + \phi(4 - W)\right]\right]\right\} = \frac{1}{N}\exp\left[2\pi i\left[\frac{n}{N}(2 - W) + \phi(2 - W)\right]\right]\left\{A°(2 - W) + A°(-W)\exp\left[-2\pi i\left[2\frac{n}{N} + (\phi(2 - W) - \phi(-W))\right]\right] + A°(4 - W)\exp\left[2\pi i\left[2\frac{n}{N} + (\phi(4 - W) - \phi(2 - W))\right]\right]\right\} \quad (12)$$

where the phases are given in fraction of 2π.

The invariance of the superstructure requires that

$$\phi(2 - W) - \phi(-W) = \phi(4 - W) - \phi(2 - W) = \phi = 2\mu/N \quad (13)$$

namely, the phases of $\mathbf{A}°(4 - W)$ and $\mathbf{A}°(-W)$ amplitudes must be equally but in oppositly related to the $\mathbf{A}°(2 - W)$ phase that can assume any value among 0 and 1 turn. Therefore

$$\mathbf{C}(n,\mu) = \frac{1}{N}\exp\left[2\pi i\left[\frac{n}{N}(2 - W) + \phi(2 - W)\right]\right]\left\{A°(2 - W) + A°(-W)\exp\left[-2\pi i\left(2\frac{n + \mu}{N}\right)\right] + A°(4 - W) \times \exp\left[2\pi i\left(2\frac{n + \mu}{N}\right)\right]\right\} \quad (14)$$

As a result, changing the phase of $\phi/2$ shifts the curvature modulus of μ base pairs along the sequence, whereas changing

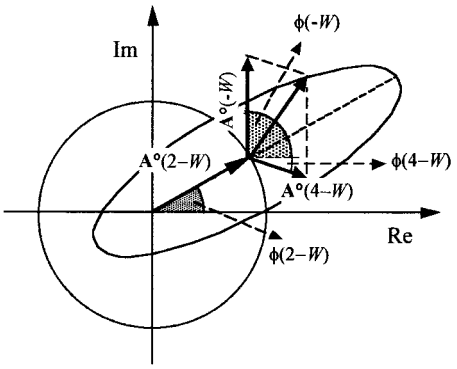

Figure 5. Representation of the dependency between the phases ϕ of the constrained amplitudes: $\phi(2 - W)$ can assume any value from 0 to 2π, whereas the other phases must equivalently change in opposite ways with respect to the first one. Therefore, for every value assumed by $\phi(2 - W)$, the vector representing the vectorial sum of $\mathbf{A}°(-W)$ and $\mathbf{A}°(4 - W)$ describes an elliptic trajectory in the complex plane.

$\phi(2 - W)$ corresponds to a coherent rotation about the helical axis, namely, to change only the phase of the curvature function; for example, a phase of 0.5 turns rotates the whole chain in such a way that the base pairs that faced in face out after the rotation.

Therefore, the phases of the constrained amplitudes do not change the superstructure as a whole (in the case of the straight DNA), but change the curvature $\mathbf{C}(n)$ along an elliptic trajectory in the complex plane whose semiaxes are the difference and the sum of the amplitudes $\mathbf{A}°(4 - W)$ and $\mathbf{A}°(-W)$ centered at the $\mathbf{A}°(2 - W)$ position. This is pictorially represented in Figure 5.

For $-1 < W < 1$, $A°(4 - W) = 0$ and the elliptic trajectory degenerates in a circle.

The length of these trajectories represents the degeneration of the ground state in terms of the writhing number. Therefore, adopting the approximate formulation of the elliptic circumference, the ground-state entropy can be expressed as

$$S°(W)/k_B = \ln\{A°(2 - W)[A°^2(-W) + A°^2(4 - W)]^{1/2}\} + \text{const.} \quad (15)$$

Consequently,

$$G°(W,\Delta L) = E°(W,\Delta L) - 1/\beta \ln\{A°(2 - W)[A°^2(-W) + A°^2(4 - W)]^{1/2}\} + \text{const.} \quad (16)$$

Figure 6 shows the good agreement between the theoretical entropy calculated with our model for the Gebe and Schurr 468 bp sequence and their Monte Carlo results.[16]

Figure 7 illustrates the elastic free energy, $G°(W,\Delta L)$, of a 468 bp DNA versus the writhing number for different ΔL (the *constant* has been set equal to zero without lacking of generality).

From $\Delta L = 0$ to $\Delta L = 1.0$ only one minimum is present corresponding to the nearly planar circular form. The first writhe transition occurs between $\Delta L = 1.25$ and 1.50 when another minimum arises corresponding to the figure-8 form. A second transition appears between $\Delta L = 2.25$ and 2.50. The free energy barriers corresponding to the two transitions are $0.5/\beta$ and $0.2/\beta$, respectively.

Figure 8 shows the distribution function versus the writhing number for linking number differences ranging from 0 to 2.5 turns with an interval of 0.25. The writhe transitions from the circle to the interwound forms, through the figure-8, are clearly reported in terms of ΔL and W.

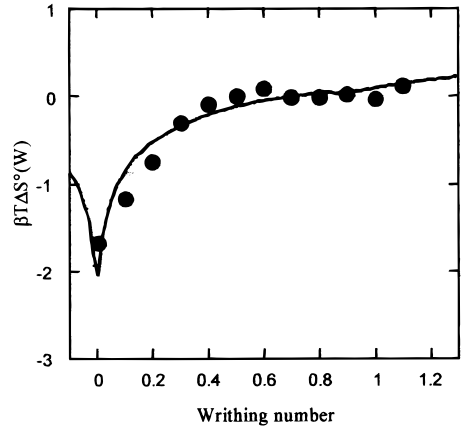

Figure 6. Theoretical entropy (solid line) of a uniform 468 bp vs the writhing number W in comparison with the Gebe and Schurr Monte Carlo simulations data[16] (●).

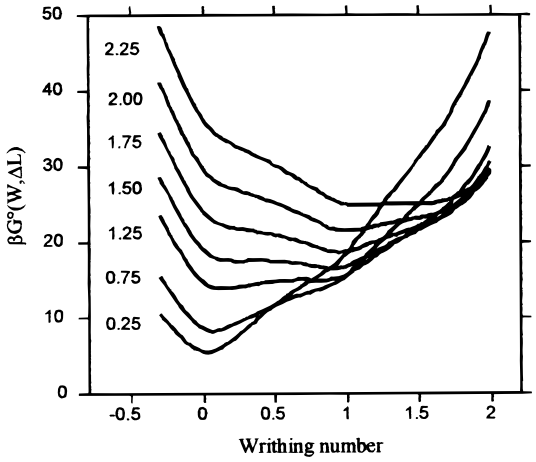

Figure 7. Elastic free energy, $G°(W,\Delta L)$, of a uniform 468 bp DNA vs the writhing number W for different linking number differences ΔL (indicated).

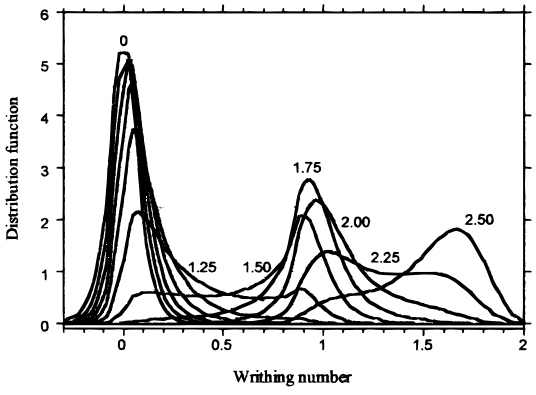

Figure 8. Probability distribution as a function of the writhing number for different linking number differences ranging from 0 to 2.50 with an interval of 0.25. The writhe transformations from the circle to the interwound figure-8 form, through the figure-8, are easily recognized and the pertinent transitions localized in terms of ΔL.

Figure 9 illustrates the good agreement between the writhing number probability distribution of the Monte Carlo data and our results for some selected linking number differences.

Finally, Figure 10 shows the ensemble average writhing number $\langle W \rangle$ and the related transformation derivative versus the linking difference; as shown in the figure, the first writhe transition occurs at $\Delta L = 1.35$ turns, in perfect agreement with

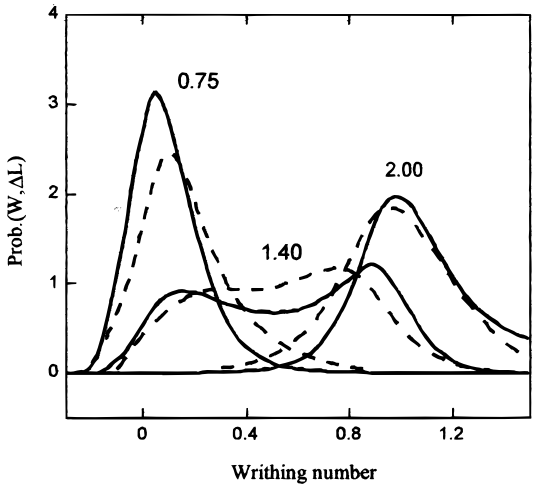

Figure 9. Comparison of the writhing number probability distribution for some selected linking number differences, between Monte Carlo data by Gebe and Schurr[16] (dashed lines) and our results (solid lines). Monte Carlo data are reported using the same smoothing function adopted for the theoretical results for a more direct comparison.

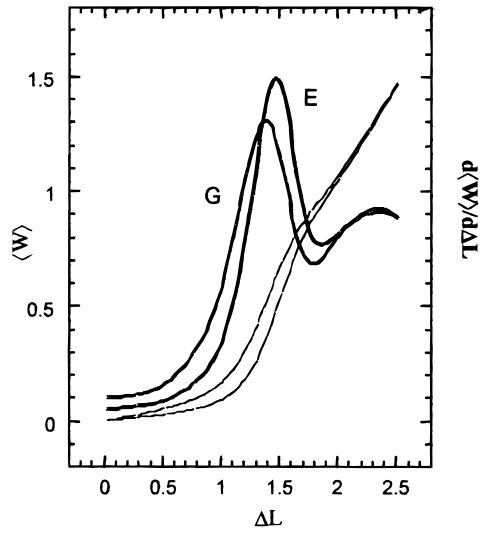

Figure 10. Ensemble average values of the writhing number $\langle W \rangle$ (solid lines) and the related derivative vs the linking difference ΔL (bold lines). The corresponding values weighted with the energy distribution instead of the free energy distribution are reported for comparison. For clarity the two averages are indicated with E and G, respectively.

the Monte Carlo simulations,[16] and a second wider writhe transition appears to rise at $\Delta L \approx 2.3$.

In order to evaluate the entropy role on the writhe transformations, it is reported for comparison the average writhing number, weighted with the energy instead of the free energy distributions. The first writhe transition shifts at $\Delta L = 1.48$, corresponding to a value of 0.13 turns, higher than that obtained taking into account the entropy contributions and in very good agreement with the Monte Carlo simulations.[16]

In fact, because of the entropy independence and the energy dependence on DNA length, the writhe transition shifts to lower ΔL values by increasing the DNA length. On the contrary, the transition is sharper and the entropy effect negligible for shorter DNAs.

It is worth noting that, neglecting the entropy, all the transitions occur at the same ΔL independently of the DNA length, according to the Le Bret mechanical model.[6,7]

Furthermore, it is easy to verify that the value $\Delta L = \sqrt{3}b/t$ found by Le Bret is perfectly justified by our model. In fact, this value does not correspond to the thermodynamic condition that the energy of the open circular form equals that of the figure-8 form but to the mechanical condition that the energy barrier vanishes. When it occurs, in the absence of thermal fluctuations, the representative point of the circle slides along the energy downhill until the other minimum at $W = 1$.

In fact, as seen before, in the interval between the circle and the figure-8 form, the energy can be expressed as

$$E^\circ(W,\Delta L) = b/(2N)[A^\circ(-W)^2 + A^\circ(2 - W)^2] + t/(2N)[2\pi(\Delta L - W)]^2 \quad (17)$$

Since the amplitudes are fitted by optimization technique with a polynomial, we can obtain the Le Bret condition as

$$\left(\frac{\partial E^\circ}{\partial W}\right)_{W=0} = \left\{\frac{1}{2N}[b(\mathrm{B} + 2\mathrm{C}W + 3\mathrm{D}W^2 + ...) - 8\pi^2 t(\Delta L - \mathrm{W})]\right\}_{W=0} = 0 \quad (18)$$

From eq 18 it easily comes out that $\Delta L = \mathrm{B}/(8\pi^2)b/t$. As we found $B = 136.5$ and ΔL is equal to 1.728, which is practically equal to the Le Bret value of $\sqrt{3}$.

However, a satisfactory evaluation of the circle−figure-8 transition ΔL can be obtained for intrinsically straight DNAs by considering the free energies of the two forms.

Recalling eq 16, the ground-state elastic free energy of the circle ($W = 0$) is

$$G^\circ(0,\Delta L) = b/(2N)(2\pi)^2 + t/(2N)(2\pi\Delta L)^2 - 1/\beta \ln(2\pi) + \text{const.} \quad (19)$$

and that of the planar figure-8 form ($W = 1$) is

$$G^\circ(1,\Delta L) = b/(2N)\, 2(2.405\pi)^2 + t/(2N)[2\pi(\Delta L - 1)]^2 - 2/\beta \ln(2.405\pi) + \text{const.} \quad (20)$$

As discussed before, we can consider the equilibrium constant of the first writhe transition as

$$K = \exp\{-\beta[G^\circ(1,\Delta L) - G^\circ(0,\Delta L)]\} \quad (21)$$

Consequently, the transition will take place when $G^\circ(1,\Delta L) = G^\circ(0,\Delta L)$. That is,

$$\Delta L = 1/2 + 0.946b/t - 0.056N/(\beta t) \quad (22)$$

where ΔL is the linking number difference between the figure-8 form and the linear form. Using the above formulation, we can evaluate the molar fraction of the figure-8 form versus the value of the twisting deformation for several DNA lengths (see Figure 11):

$$x(8) = \frac{K}{1 + K} \quad (23)$$

It is interesting that in the limit case of $b/t = 0$, and contrary to the Le Bret formulation, the transition is correctly predicted to occur at $\Delta L = 1/2$, when the entropy contribution (the last term in eq 22) can be neglected (this is true for the purely mechanical model).

Finally, it is interesting that the ΔL values of the first writhe transition obtained by Schlick et al.[12] using Monte Carlo simulations for an elastic constant ratio equal to 1.0 and 1.5, are in perfect agreement with our formulation. Considering that

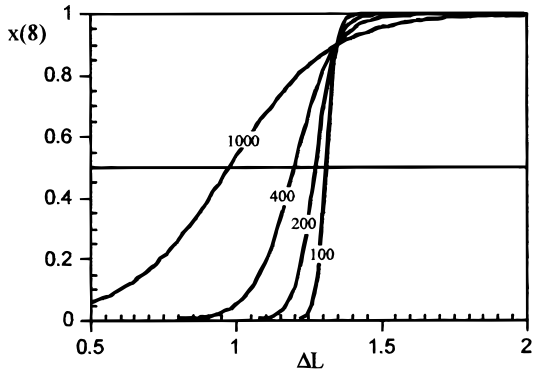

Figure 11. Molar fraction of the figure-8 form vs the linking number difference, ΔL, for straight DNAs with different number of base pairs and assuming integral intrinsic twisting numbers.

their results concern the minimum energy structures rather than ensembles, a reduced eq 22 must be used, neglecting the term $0.056N/(\beta t)$.

Evaluation of the Canonical Partition Functions and Thermodynamic Functions for Writhe Transformations

To justify the apparent equivalence of the thermal fluctuations, we have evaluated the canonical partition function in terms of the linking and writhing numbers for low writhing forms. In fact, fixing the linking and the writhing number is equivalent to topologically defining a superstructure ensemble. First of all, consider the equilibrium constant between two given writhe states of DNA W and $W^{\#}$, characterized by the same ΔL. This can be expressed as

$$K = \frac{q(W,\Delta L)}{q(W^{\#},\Delta L)} \exp[-\beta(G^{\circ}(W,\Delta L) - G^{\circ}(W^{\#},\Delta L))] \quad (24)$$

where the free energy terms both refer to the ground states of the circular forms, evaluated with respect to the same intrinsic linear form, which implicitly take into account the degeneration. In classical statistical mechanics, all kinetic contributions completely cancel in the ratio of the partition function; consequently there just remains the ratio of the configuration integrals. Let $q(W,\Delta L)$ be the configurational canonical molecular partition function of the DNA in terms of its writhing number W and linking number difference ΔL:

$$q(W,\Delta L) = \sum g(W) \exp(-\beta \Delta E(W,\Delta L)) \quad (25)$$

where the summation is extended to the states with fixed W and ΔL and $g(W)$ represents their degeneration.

Supposing in a first approximation the independence between twisting and bending elastic energy contributions, we can factorize the configurational canonical partition function of a circular DNA as

$$q(W,\Delta L) = q_b(W)\, q_t(W,\Delta L) \quad (26)$$

This corresponds to neglect of eventual coupling between bending and twisting energy within the dinucletide steps, so that $\Delta E = \Delta E_b + \Delta E_t$.

Setting for the sake of clarity, the deviation of the amplitudes from the constrained values, $\Delta \mathbf{A_j} = \mathbf{A}(j - W) - \mathbf{A}^{\circ}(j - W)$ and $b = \beta b/(2N)$,

$$q_b(W) = \sum g(W) \exp(-\beta \Delta E_b) = \sum g(W) \exp(-b \sum_j \Delta A_j^2) \quad (27)$$

where ΔA_j represents the fluctuations of the corresponding amplitudes.

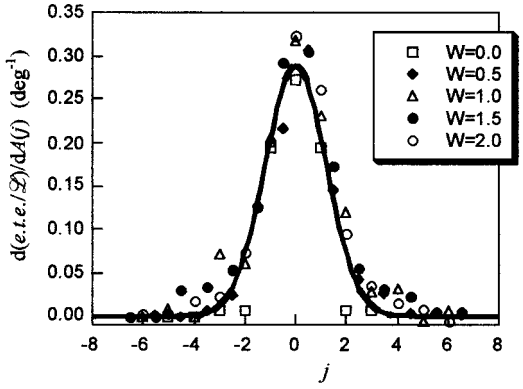

Figure 12. Gradient components of the end-to-end distance normalized with the contour length, for 10° increments of the $\mathbf{A}(j)$ amplitudes. The symbols refer to some forms with different writhing numbers; the solid line is the fitting Gaussian.

Substituting summations with integrals,

$$q_b(W) = \prod \frac{1}{\sigma} \int \exp(-b\Delta A_j^2)\, d\Delta \mathbf{A}_j \quad (28)$$

where $1/\sigma$ is the integration factor whose value is unessential, as will be seen in the following; that is, σ represents the ΔA_j unit increment. Equation 28 is transformed as

$$q_b(W) = \prod_j \frac{1}{\sigma} \int_0^{2\pi} d\phi_j \int_0^{\Delta A_j^M} \exp(-b\Delta A_j^2) d\Delta A_j = \prod_j \left(\frac{\pi}{b\sigma}\right) \{1 - \exp[-b(\Delta A_j^M)^2]\} \quad (29)$$

where ΔA_j^M is the maximum deviation from the ground-state amplitudes.

In order to evaluate the limits of the fluctuations for the different $\Delta \mathbf{A_j}$ amplitudes, the breaking of the circularization, resulting from an increment (10 degrees) of each amplitude, was calculated as the derivative of the end-to-end distance with respect to A_j.

As a result, the same Gaussian-like curve in function of the frequency j is obtained for the circular, the figure-8, and the interwound figure-8 forms (see Figure 12).

Therefore, except for the frequencies in a strict region of k $(-2, +2)$, the other j amplitudes practically fluctuate independently.

Consequently, the maximum of the fluctuation ΔA_j^M for the unconstrained amplitudes is large enough to make insignificant the exponential with respect to the unit. As a result, for these amplitudes,

$$q_b^{(j)}(W) \rightarrow \left(\frac{\pi}{b\sigma}\right) = \left(\frac{2\pi N}{\beta b \sigma}\right) \quad (30)$$

However, in the case of the kth frequencies within the region of constrained amplitudes, the ΔA_j^M values are severely restricted in their fluctuations and assume values in a strict interval around those characterizing the ground state.

Furthermore, as the diagram in Figure 12 is practically independent of writhing, all the contributions to $q_b(W)$ are equal for any value of W and cancel in the ratio of eq 24.

Similarly, we can obtain the twist partition function:

$$q_t(W,\Delta L) = \sum g(W,\Delta L)\exp(-\beta E_t) = \sum g(W,\Delta L)\exp(-t\sum_j \Delta B_j^2) \quad (31)$$

where $t = \beta t/(2N)$ and ΔB_j represent the twist fluctuations.

As in the case of the bending partition function, eq 31 can be transformed as

$$q_t(W,\Delta L) = \prod_{j\neq 0}\left(\frac{\pi}{t\delta}\right)\{1 - \exp[-t(\Delta B_j^M)^2]\} \quad (32)$$

$\mathbf{B}_j$ is the jth term of the Fourier series of the twist distribution along the sequence and $1/\delta$ is the integration factor. In this case, for a given ΔL and W, only the amplitude with $j = 0$ is topologically fixed and equal to $2\pi(\Delta L - W)$. Therefore, all the Fourier modes are free to fluctuate independently of the writhing number except that with $j = 0$. Consequently, all the contributions to $q_t(W,\Delta L)$ cancel in the ratio of eq 24, which becomes

$$K = \frac{g^\circ(W)}{g^\circ(W^\#)}\exp\{-\beta[E^\circ(W,\Delta L) - E^\circ(W^\#,\Delta L)]\} \quad (33)$$

where the degenerations $g^\circ(W)$ and $g^\circ(W^\#)$ refer to the ground states of the corresponding forms, which demonstrates the main issue of this section. Grouping all the exponential terms that contribute to the ground-state energy difference ΔE° and rearranging eq 33,

$$-\ln K = \beta\Delta E^\circ - \ln\frac{g^\circ(W)}{g^\circ(W^\#)} \quad (34)$$

ΔE° contains both twisting and bending contributions. As discussed before, they can be easily found from eq 10 considering the constrained Fourier terms only (indicated in Figure 2) and $\Delta B(0) = 2\pi(\Delta L - W)$ (the other terms vanishes).

The last term in eq 34 represents the ground-state entropy difference, in k_B units, that only depends on the writhe and, contrary to the energy, is independent of the DNA length.

This means that the energy term dominates for DNAs with a few hundred base pairs, whereas the entropy term becomes more and more important for longer sequences.

A Model for the Sequence-Dependent Writhe Transitions in Circular DNAs

In the previous section, we presented a model for the writhe transitions for a hypothetical straight DNA characterized by an intrinsic zero curvature, namely, by Fourier amplitudes all identically zero.

However, a natural DNA is characterized by a sequence-dependent curvature that can be represented by the pertinent curvature function along the sequence. Its spectrum is generally characterized by nonzero amplitudes contrary to the straight DNA.

To evaluate the intrinsic curvature of a DNA sequence as given in eq 1, we have adopted our set of roll and tilt angles that define the deviation vector $\mathbf{d} = \rho - i\tau$ as well as the corresponding twist angles Ω. These are reported in Table 1 for the 16 different dinucleotide steps as obtained in a first approximation by energy minimization procedures and refined to fit electrophoretic experiments of a very large set of DNA tracts.[23,25−27]

TABLE 1: d, Ω[a]

	A	T	G	C
T	(8.0, 0.0), 34	(−5.4, −0.5), 36	(6.8, 0.4), 34	(2.0, −1.7), 35
A	(−5.4, 0.5), 36	(−7.3, 0.0), 35	(1.0, 1.6), 34	(−2.5, 2.7), 34
C	(6.8, −0.4), 34	(1.0, −1.6), 34	(4.6, 0.0), 34	(1.3, −0.6), 33
G	(2.0, 1.7), 35	(−2.5, −2.7), 34	(1.3, 0.6), 33	(−3.7, 0.0), 33

[a] $\mathbf{d} = (\rho,-\tau)$ and Ω in degrees.

These parameters work very satisfactorily in predicting the sequence-dependent circularization propensity in excellent agreement with the experimental data.[35]

If we adopt for a curved DNA the values of the constrained amplitudes found in the case of the straight DNA (see Figure 2), the resulting superstructure will not generally assume a closed circular form because of the contribution of the remaining unconstrained amplitudes. However, if one considers the gradient of the end-to-end distance consequent to the changes of the different amplitudes (see Figure 12), one can realize that a slight refining of the constrained amplitudes is enough to reach the correct circularization because of their high degree of coherence and effectiveness in sealing the DNA strands.

This corresponds to slightly modifying the amplitudes in a very limited range of frequencies to eliminate the end-to-end distance.

The phases that are free to change independently remain those of the intrinsic linear form: this ensures the minimization of the bending energy. However, for $|W| > 1$ the relations among the phases of the amplitudes $\mathbf{A}^\circ(2 - W)$, $\mathbf{A}^\circ(4 - W)$, and $\mathbf{A}^\circ(-W)$, as already discussed, should be taken into account in the minimization of the bending energy; this is easily obtained by steepest descent methods. As a result, most of the intrinsic conformational features remain practically invariant.

As for the straight DNA, also for sequence-dependent curved DNAs the thermal fluctuations can be considered practically equivalent for low writhing DNAs or for superstructures whose writhing numbers differ less than ± 1. Therefore, the free energy variation versus the writhing number contains only the ground-state energy and entropy terms.

While the ground-state energy can be easily evaluated, as in the case of the straight DNA using eq 10, the entropy requires further considerations.

In this case the ground-state degeneration is not simply evaluated from the length of the trajectory in the complex plane because the bending energy, contrary to the straight DNA, is now dependent on the phases.

In fact, the constrained amplitudes are polarized in the direction of the corresponding amplitudes of the intrinsic linear form; as a consequence the phase degeneration is restricted depending on the product of the moduli of the circular and linear Fourier terms (paper in preparation).

Therefore the evaluation of the entropy is more difficult; nevertheless it can be expressed analytically. However, the general result is that the role of the entropy in the writhe transformations of curved DNAs is less important than that for a straight DNA with the same length.

Some Results on Sequence-Dependent Writhe Transformations

The model we have illustrated appears to be satisfactorily reliable to predict writhe transformations of circular (or looping) DNAs, as demonstrated by the striking agreement with Monte Carlo simulations.

Adopting this model, we have estimated the writhe transitions of curved DNAs. All the calculations were made using the

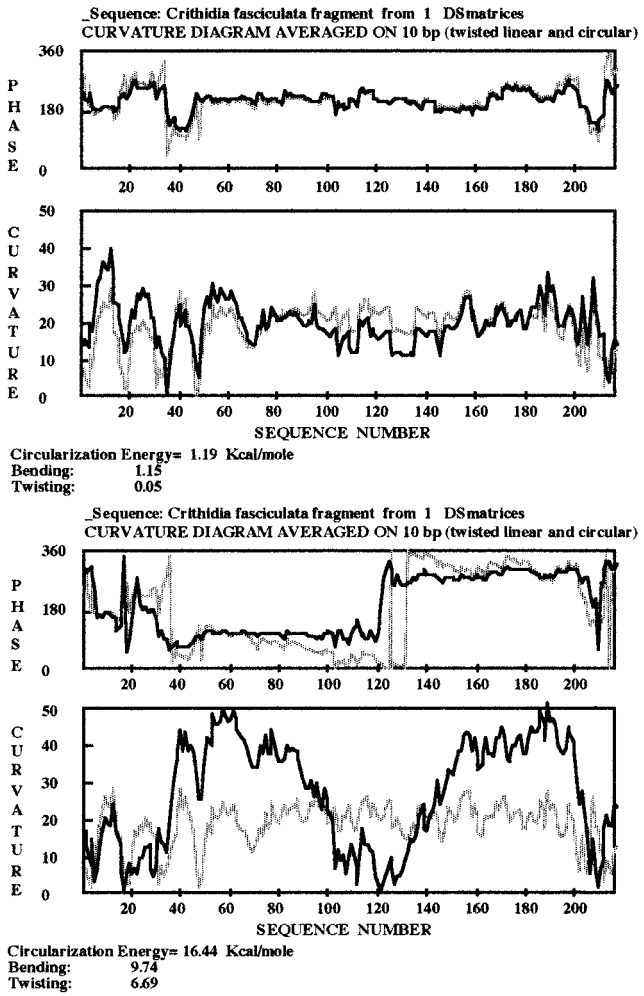

Figure 13. Curvature diagrams representing the moduli and the phases (black lines) of the open circular (top) and the figure-8 (bottom) forms for the 217 bp DNA sequence containing the loop region of *Crithidia fasciculata*. The moduli are reported in degrees per turn of a double helix. The phases are reported in degrees. The ground-state energy contributions are indicated. The gray lines represent the curvature functions of the forms obtained from the linear intrinsic structure by twisting its local axes to obtain the same linking number for the two final forms.

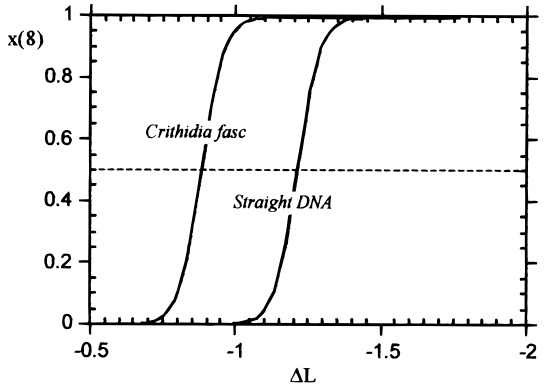

Figure 14. Molar fraction of figure-8 form vs the linking number difference, ΔL, for the loop region of *Crithidia fasciculata*, as compared to that of an intrinsically straight DNA with the same length and intrinsic twist.

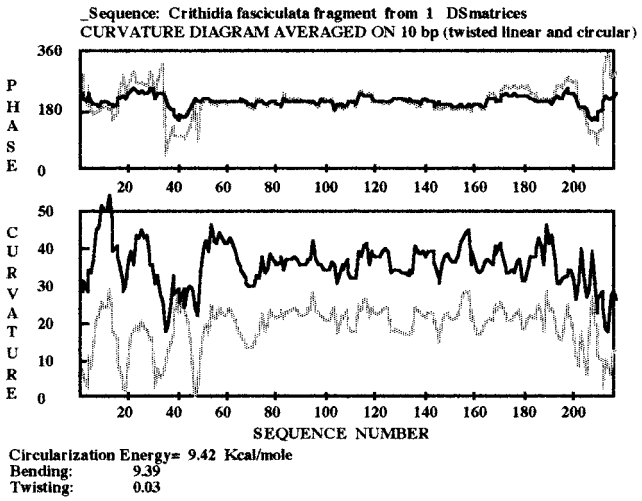

Figure 15. Curvature diagram representing the moduli and the phases (black lines) of the toroidal form ($W = 1$) for the same sequence of Figure 13. The moduli are reported in degrees per turn of a double helix. The phases are reported in degrees. The ground-state energy contributions are indicated. The gray lines represent the curvature function of the linear intrinsic twisted structure.

elastic parameters ($P = 450$ Å and $C = 2.1 \times 10^{-19}$ erg cm) previously adopted with success in predicting the sequence-dependent DNA circularization propensity.[22] The computer program is available on the Internet at http://magritte.phys.uniroma1.it/researches.html.

Figure 13 shows the curvature diagrams of the open circular and the figure-8 minimum energy forms compared with those of the intrinsic linear form for a 217 bp DNA tract containing the loop region of *Crithidia fasciculata*.

Figure 14 illustrates the molar fraction of the figure-8 form with respect to the circle versus ΔL. The first transition is strongly shifted at $\Delta L = 0.9$. It is useful recalling that changing ΔL really means changing the intrinsic twist, e.g., by intercalating dyes, interactions with unwinding proteins, modification of the water activity, etc.

It is noteworthy that the minimum energy superstructure with $W = 1$ corresponds to a toroidal structure (whose curvature diagram is reported in Figure 15) practically equal to that found by Tan et al. using molecular dynamics simulations.[32] However, this structure has a different linking number with respect to the figure-8 form, and they cannot interconvert each other by writhe transformations; for this reason, this form must not be considered in the writhe equilibria.

Some particular structures may be more stable in a supercoiled form even in the absence of an external twisting deformation. An example is given by the Koo et al. sequence A4N6 $((AAAACGGGCC)_n)$,[33] which, due to its intrinsic superhelical structure, appears to be more stable in the figure-8 form than in the open circular form when $n > 29$ (see Figure 16).

The transition from the circle to the figure-8 form can be also influenced by the presence of bending-inducing proteins like CAP. As we did in the case of circularization, we consider the effect of the protein as a modification of the intrinsic curvature of the DNA chain. This is obtained by imposing a bend of 90°[34] to the protein-binding domain, as described in a previous paper.[23]

As an example, we illustrate the case of the 434 bp sequence of the *E. coli uxuAB* operon regulatory region (EMBL n. X03411) containing the CAP consensus sequence. The transition profiles in the absence and in the presence of CAP are reported in Figure 17; the profile of a straight sequence of the same length is also given for comparison. Figures 18 and 19

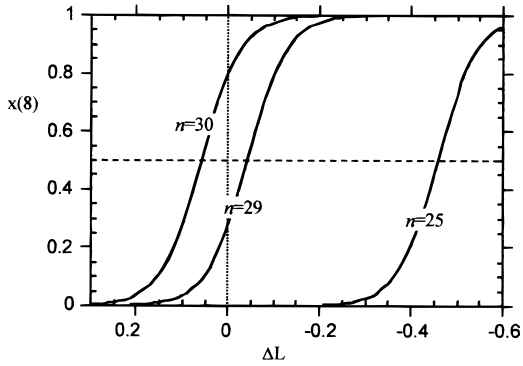

Figure 16. Molar fraction of figure-8 form vs the linking number difference, ΔL, of the Koo et al.[33] multimeric DNA A4N6 ($(AAAACGGGCC)_n$) for $n = 25$, 29, and 30.

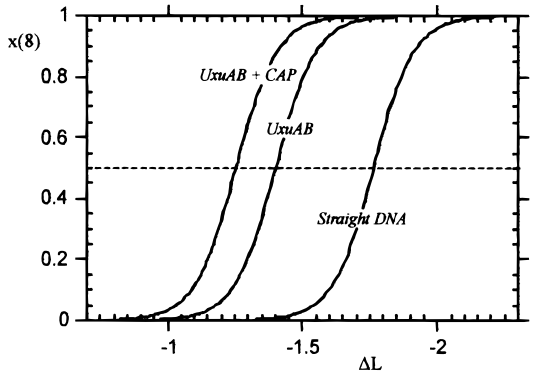

Figure 17. Molar fraction of figure-8 form vs the linking number difference, ΔL, for the sequence of the *E. coli uxuAB* operon regulatory region in the absence and in the presence of CAP, compared to that of an intrinsically straight DNA of the same length and intrinsic twist.

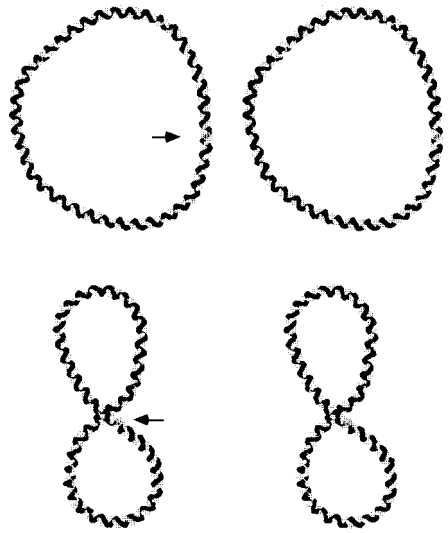

Figure 18. Stereoprojections of the superstructures representing the ground state of the open circular and the figure-8 forms of the *E. coli uxuAB* operon regulatory region. The arrows indicate the origin of the sequence.

show the structures of the corresponding forms. It is noteworthy that CAP binding produces besides the shift of the transition in writhe a different crossing of the figure-8 forms in order to segregate the tracts with the higher curvature at the loop regions. This sequence-dependent effect could be relevant for the control of gene expression that depends on bringing together determined DNA tracts often distant along the sequence.

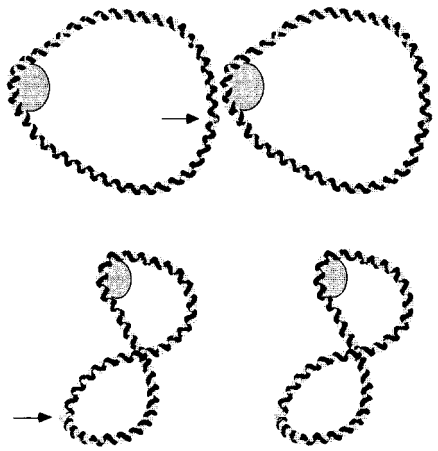

Figure 19. Stereoprojections of the superstructures representing the ground state of the circular and the figure-8 forms of the *E. coli uxuAB* operon regulatory region distorted by a CAP protein virtually bound to the consensus sequence; CAP is schematically represented as a gray oval. Note the different crossing region of the figure-8 form with respect to that of Figure 18. The arrows indicate the origin of the sequence.

Conclusions

Physical phenomena are always the result of a huge number of causes that affect them to some extent; however, sometimes it is possible to individuate a single cause that dominates over the others. This allows us to find relatively simple explanations of the experimental data and predict the results of new observations. The main conclusion of this paper is that the DNA deformation from its intrinsic superstructure, evaluated adopting a first-order elasticity model,[23−27] appears to be the driving effect to explain the sequence-dependent superstructural transformations of DNAs.

Although the model we propose in the present paper contains several approximations and physical assumptions, it has the advantage of being flexible and widely applicable. These features probably make it more useful than Monte Carlo simulations that are restricted to rather ideal cases of wormlike DNAs or DNAs containing some hypothetical bends. Moreover, the mathematical structure of our model allows an easy advancement toward a more rigorous solution by improving the elastic model, i.e., introducing some coupling between bend and twist or a sequence-dependent differential flexibility, or extending it to higher writhing densities and branched supercoiling.

An extension of our model to problems of biological relevance could be the study of the transcription loop stability as a function of the sequence and how it is influenced by the binding of regulatory proteins. In fact DNA loops have been demonstrated to mediate transcription, activation, and repression in many systems,[3,4] so that sequence effects may play an important role in their stabilization and regulation. For this reason, the model could be adopted to predict allosteric effects in topologically constrained DNAs, namely, changes of the protein-binding constants induced by the presence of bending or unwinding moieties, including the nucleosomes (paper in preparation), as well as to evaluate the role of the curvature as a factor controlling the biological mechanism of the loop formation in DNAs.

Finally, it is worth noting that our model generally requires about 1 s of CPU time on a personal computer, while Monte Carlo simulations need days on larger computers.

Acknowledgment. This research was supported by CNR "Progetto Finalizzato Chimica Fine" and "Progetto Strategico Biologia Strutturale".

Appendix

As reported in previous papers,[23,26] in the case of an intrinsically straight DNA (corresponding to all the $A(j) = 0$) the circularization conditions for the ground-state circular form in the Fourier space are rather simple. They imply $A(0) = 2\pi$, corresponding to the sum of all curvatures on the average plane.

In the figure-8 form ($W = 1$) the minimum number of constrained amplitudes implies $A(+1) = A(-1) = 2.405\pi$ (this corresponds to the first zero of the zero-order Bessel function, as will be explained below).

In fact, since the figure-8 form lies in a plane, it must contain equivalent contributions from the 1 and -1 Fourier modes. Consequently, the curvature function we obtain is

$$\mathbf{C}(n) = \frac{1}{N}\left[\mathbf{A}(1)\exp\left(2\pi i\frac{n}{N}\right) + \mathbf{A}(-1)\exp\left(-2\pi i\frac{n}{N}\right)\right] = \frac{2}{N}A(\pm 1)\cos\left(2\pi\frac{n}{N} + \phi\right) \quad \text{(i)}$$

where ϕ is the mean between the phases of the $\mathbf{A}(1)$ and $\mathbf{A}(-1)$ amplitudes. Let $\phi = \phi' + \pi/2$; at the limit of a continuous chain, the integral curvature at the sequence position n is

$$\mathbf{C}(n) = \frac{1}{N}\int_0^n 2A(\pm 1)\sin\left(2\pi\frac{m}{N} + \phi'\right) dm = \frac{A(\pm 1)}{\pi}\left[\cos\phi' - \cos\left(2\pi\frac{n}{N} + \phi'\right)\right] \quad \text{(ii)}$$

The condition of the ring closure is found by imposing equal to zero the summation in the complex plane of the vectors representing the unit segments of the chain. At the limit of a continuous chain, it must be

$$\int_0^N \exp(i\mathbf{C}(n))\, dn = 0 \quad \text{(iii)}$$

Equation iii can be related to the integral form of the Bessel functions; in fact, it is easy to see that the solution corresponds to the first zero of the zero-order Bessel function:

$$J_o(A(\pm 1)/\pi) = 0 \quad \text{(iv)}$$

That occurs for $A(\pm 1) = 2.405\pi$ (corresponding to the $A(2 - W)$ and $A(-W)$ Fourier terms when $W = 1$). In the case of the planar interwound figure-8 form, the sum of all the curvatures (namely, $A(0)$, when $W = 2$) is as for the circle equal to 2π. On the contrary, the $A(-2)$ and $A(+2)$ (corresponding to $A(-W)$ and $A(4 - W)$) are both equal to 2.41π. This corresponds to the minimum value for the $A(-2)$ and $A(+2)$ Fourier modes, which allows the helical axis of DNA to double cross. These structures do not take into account the excluded volume at the crossing points, but represent useful models for obtaining more realistic forms by steepest descent algorithms (see text).

References and Notes

(1) Fuller, F. B. *Proc. Natl. Acad. Sci. U.S.A.* **1971**, *68*, 814−819.
(2) Crick, F. H. C. *Proc. Natl. Acad. Sci. U.S.A.* **1976**, *73*, 2639−2643.
(3) Ptashne, M. *Nature* **1986**, *322*, 697−701.
(4) Gralla, J. D. *Cell* **1989**, *57*, 193−195.
(5) Benham, C. *J. Proc. Natl. Acad. Sci. U.S.A.* **1977**, *74*, 2397−2401.
(6) Le Bret, M. *Biopolymers* **1979**, *18*, 1709−1725.
(7) Le Bret, M. *Biopolymers* **1984**, *23*, 1835−1867.
(8) Shimada, J.; Yamakawa, H. *J. Mol. Biol.* **1985**, *184*, 319−329.
(9) Levene, S. D.; Crothers, D. M. *J. Mol. Biol.* **1986**, *189*, 73−83.
(10) Olson, W. K. *Curr. Opin. Struct. Biol.* **1996**, *6*, 242−256.
(11) Hao, M. H.; Olson,W. K. *Macromolecules* **1989**, *22*, 3292−3303.
(12) Schlick, T.; Olson, W. K.; Westcott, T.; Greenberg, J. P. *Biopolymers* **1994**, *34*, 565−597.
(13) Westcott,T. P.; Tobias, I.; Olson, W. K. *J. Phys. Chem.* **1995**, *99*, 17926−17935.
(14) Bauer, W. R.; Lund; R. A.; White; J. H. *Proc. Natl. Acad. Sci. U.S.A.* **1993**, *90*, 833−837.
(15) White, J. H.; Lund, R. A.; Bauer, W. R. *Biopolymers* **1996**, *38*, 235−250.
(16) Gebe, J. A.; Schurr, J. M. *Biopolymers* **1996**, *38*, 495−503.
(17) Sprous, D.; Tan, R. K. Z.; Harvey, S. C. *Biopolymers* **1996**, *39*, 243−258.
(18) Marko, J. F.; Siggia, E. D. *Science* **1994**, *265*, 506−508.
(19) Laundon, C. H.; Griffith, J. *Cell* **1988**, *52*, 545.
(20) Lobel, R. B.; Schleif, R. F. *Science* **1990**, *250*, 528−532.
(21) Klenin, K. V.; Frank-Kamenetskii, M. D.; Langowski, J. *Biophys. J.* **1995**, *68*, 81−88.
(22) Chirico, G.; Langowski, J. *Biophys. J.* **1996**, *71*, 955−971.
(23) De Santis, P.; Fuà, M.; Savino, M.; Anselmi, C.; Bocchinfuso, G. *J. Phys. Chem.* **1996**, *100*, 9968−9976.
(24) De Santis, P.; Palleschi, A.; Savino, M.; Scipioni, A. *Biophys. Chem.* **1988**, *32*, 305−317.
(25) Boffelli, D.; De Santis, P.; Palleschi, A.; Scipioni, A. *Int. J. Quantum Chem.* **1992**, *42*, 1409−1426.
(26) De Santis, P.; Fuà, M.; Palleschi, A.; Savino, M. *Biophys. Chem.* **1995**, *55*, 261−271.
(27) De Santis, P.; Palleschi, A.; Savino, M.; Scipioni, A. *Biochemistry* **1990**, *29*, 9269−9273.
(28) Bracewell, R. In *The Fourier Transform and Its Applications*; McGraw-Hill Book Co.: New York, 1965.
(29) Calagareanu, G. *Czech. Math. J.* **1961**, *11*, 588−593.
(30) Spiegel, M. R. In *Fourier Analysis*; McGraw-Hill Book Co.: New York, 1974.
(31) Vologodskii, A. V.; Levene, S. D.; Klenin, K. V.; Frank-Kamenetskii, M. D.; Cozzarelli, N. R. *J. Mol. Biol.* **1992**, *227*, 1224−1243.
(32) Tan, R. K. Z.; Harvey, S. C.; Di Mauro, E.; Camilloni, G.; Venditti, P. *J. Biomol. Struct. Dynam.* **1996**, *13*, 855−872.
(33) Koo, H. S.; Wu, H. M.; Crothers, D. M. *Nature* **1986**, *320*, 501−503.
(34) Schultz, S. C.; Shields, G. C.; Steitz, T. A. *Science* **1991**, *253*, 1001−1007.
(35) Kahn, J. D.; Crothers, D. M. *Proc. Natl. Acad. Sci. U.S.A.* **1992**, *89*, 6343−6347.